coatings

MDPI

Communication

Blast Resistance of a Masonry Wall Coated with a Polyurea Elastomer

Xudong Zu, Taian Chen, Youer Cai, Zhengxiang Huang and Qiangqiang Xiao *

School of Mechanical Engineering, Nanjing University of Science and Technology, Nanjing 210094, China
* Correspondence: xiao_wawj@njust.edu.cn; Tel.: +86-13701459567

Abstract: The coating of polyurea elastomers on walls is a hotspot in the protection field. This work combines a numerical simulation with experimental validation to examine the blast resistance after coating a polyurea elastomer on a 370 mm wall under a contact explosion. Firstly, the failure limit, failure mode, and failure mechanism of the 370 mm unreinforced wall under different strength loads are studied. In the case of the contact explosion, the increase in size of the 370 mm wall blasting pit gradually stops after the dose is increased to more than 1 kg. Thereafter, the energy of the explosive load wis released by splashing wall fragments as well as by the deflection and movement of the wall. Spraying double-sided polyurea reinforcement on the wall can effectively improve the resistance to damages caused by exposure to explosive loads and can inhibit the damage to the surrounding personnel and equipment caused by flying structural debris. When the polyurea thickness on the front surface is 6 mm, the optimal thickness of the back surface should be 2 mm.

Keywords: masonry wall; polyurea elastomer; blast resistance; explosive loads

Citation: Zu, X.; Chen, T.; Cai, Y.; Huang, Z.; Xiao, Q. Blast Resistance of a Masonry Wall Coated with a Polyurea Elastomer. *Coatings* **2022**, *12*, 1744. https://doi.org/10.3390/coatings12111744

Academic Editor: Enrico Quagliarini

Received: 8 September 2022
Accepted: 17 October 2022
Published: 14 November 2022

1. Introduction

Terrorist acts on buildings have never disappeared in the modern world, where they routinely take place. Clay bricks are still a major component of modern buildings. Under detonation loading, the walls will suffer extensive damage. The lives of those residing in the buildings will be gravely affected when a large avalanche develops on the back of a wall. Therefore, it is vital to research ways to improve the anti-explosion performance of the walls without altering the building's fundamental design. According to Proter et al. [1], polyurea possesses excellent impact and rear resistance, as well as great application potential for anti-terrorism and explosive protection scenarios. Moreover, polyurea elastomers can strengthen a wall via spraying, and polyurea can cure and harden quickly, which is convenient during construction [2]. According to Bahei-El-Din et al. [3] and Tekalur et al. [4], spraying polyurea on a wall helps decrease the secondary damage produced by the wall's collapse by absorbing the shock energy. The impact of the polyurea and glass fiber-reinforced polymer (GFRP)-strengthened walls on the blast resistance was examined by Hrynyk and Myers [5]. The outcomes demonstrated that the wall reinforced with polyurea was the most efficient in lowering wall deflection and enhancing energy dissipation.

Researchers from around the world have studied wall blast resistance performance in an effort to reduce the damage caused by explosions to walls. Aghdamy et al. [6] studied the characteristics of the failure and collapse of concrete masonry walls reinforced by a nanoparticle polymer and aluminum foam under dynamic and impact conditions by combining experiments and simulations. Davidson et al. [2,7] analyzed the blast-resistant mechanism of a sprayed polyurea elastomer in strengthening masonry walls through a detonation test. Gattesco et al. [8] conducted experiments and numerical studies on the non-planar behavior of reinforced masonry walls. Fan et al. [9] simulated the response of and damage to brick-filled walls under explosive loads and reported multiple failure modes of masonry walls under different proportional distances. Zheng [10] studied the

responses of non-porous masonry walls under explosive loads. Xu and Lu [11] simulated the explosive shock behavior of reinforced concrete walls and found that wall caving may be considerably reduced in concrete walls by strengthening the back surface. By simulating the enhancement effect of polymers on the masonry wall performance, Aghdamy et al. [5] drew the conclusion that polymers can significantly increase the resistance of masonry walls to explosive loads. Dinan et al. [12] determined the damage mechanism and conducted experimental research on coated polymer masonry walls. The results showed that the polymer coatings can significantly enhance the explosion-proof performance of the masonry walls. Zhu et al. [13] developed a detailed micro-numerical model that can predict the non-linear dynamic responses of both unreinforced clay brick masonry walls and polyurea-reinforced clay brick masonry walls under close-in blasting. Davidson et al. [2,7] carried out a series of field explosion experiments to investigate the blast resistance performance of a wall enhanced with polyurea. Iqbal et al. [14] conducted an experimental investigation on a coated polymer masonry wall to identify the damage mechanism. The outcomes demonstrated that the masonry wall's performance as an explosion-proof barrier was greatly improved by the coated polymer layer.

In our previous study [15], we found that the blast resistance can be strengthened by coating polyurea elastomer on a 240 mm wall through an experiment and numerical simulation, and showed that the reinforced wall will not collapse even if the wall is penetrated. In addition, the influence of the thickness of the coated polyurea on the blast resistance ability was analyzed, and the optimal structure was found. In this paper, the same research method was used to study a 370 mm wall. It was found that the coated polyurea elastomer protected the 370 mm wall, as the main load-bearing structure of the buildings, from penetrating damage and large-sizes cracks, and we also found the best structure. A 370 mm wall and 240 mm wall will be different in a building, and the destruction forms in the building will also be different. The purpose of the study was to prevent a 240 mm wall coated with a polyurea elastomer from collapsing during explosion and a 370 mm wall coated with a polyurea elastomer from penetrating damage. In summary, the combination of the research results from the two articles can provide a basis for how to enhance the responses of existing building targets to terrorist explosion damage.

2. Numerical Simulation

2.1. Blast-Resistant Performance of Clay Masonry Wall under Contact Explosion

In this section, the damage to the masonry wall under contact explosions with different quality charges is analyzed via numerical simulation.

2.1.1. Simulation Model

The masonry wall was described using a different model. The bricks and mortar were created from several material units and were viewed as separate parts in the solution. The simulation was conducted in accordance with the masonry regulations for masonry walls in the relevant standard GB 50003-2011, Code for the Design of Masonry Structures [16]. In the model, the masonry method is "one straight, one horizontal, and one cement mortar joint". The LS-DYNA finite element dynamic analysis software was used to simulate the damage effect of the entire TNT explosion on the wall. For the bricks and mortar we used the Lagrange algorithm, and for both explosives and air we used the ALE algorithm. The size of the single masonry wall was 1990 mm × 1260 mm × 370 mm. Given that the single wall was axisymmetric, a 1/2 model of the masonry wall was used for calculation. The 1/2 model of the masonry wall is shown in Figure 1.

In actual brick wall buildings, the foundation is generally excavated. The walls are built from about 0.5 m below the ground, and the masonry is firmly connected to the ground. Therefore, the part of the wall bottom close to the ground can be regarded as fully constrained during the numerical simulation modeling. There are tie bars on both sides or columns connected with the wall on the side, which can effectively limit the displacement and deformation of the wall. In order to make the wall flat and beautiful

during construction, a thin layer of low-strength mortar (M5 and below) is often used to level the outside. In order to correspond to the actual situation, a full-constraint longitudinal strip is applied to the back burst surface of the 1/2 model to simulate the supporting effect of the adjacent walls on the masonry walls, so that the constraints on both sides of the wall are stronger than those on the upper and lower sides. The constraints in the X-axis direction are imposed on the symmetry plane, and non-reflective boundaries are imposed around the air domain (except for the symmetry plane). Due to the low strength and thin thickness of the plastering mortar outside the wall, its anti-explosion effect in the contact explosion is ignored.

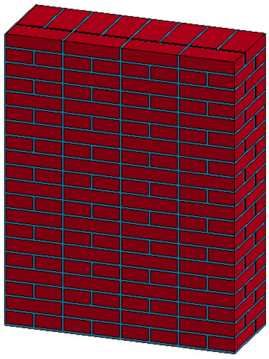

Figure 1. The 1/2 model and mesh generation of the masonry wall.

Since the duration of the explosion is very short, it is assumed that the clay brick block and mortar are well connected; that is, they are modeled in joint mode. In order to simulate the bonding, separation, and sliding between the bricks and mortar and to simulate the tensile failure and shear failure between the contact surfaces, TNTS is used to express the above relationship. The contact keyword is: * CONTACT_TIEBREAK_SURFACE_TO_SURFACE. The failure conditions of this keyword are:

$$\left(\frac{|\sigma_n|}{[\sigma_N]}\right)^2 + \left(\frac{|\sigma_s|}{[\sigma_S]}\right)^2 \geq 1 \tag{1}$$

where σ_n and σ_s are the calculated normal stress and calculated shear stress on the contact surface, respectively; $[\sigma_N]$ and $[\sigma_S]$ are the allowable normal stress and allowable shear stress on the contact surface, respectively, which can be taken as the elastic tensile strength and shear strength of the mortar material. As the tensile and shear strength between the masonry block and mortar of the brick masonry wall are relatively small, the allowable normal stress and allowable shear stress on the contact surface are 0.12 MPa and 0.14 MPa, respectively. After the failure of the contact surface, there will be dislocation and slippage between the block and mortar. At this time, the friction will prevent both from sliding. When the contact surface is dry, the friction coefficient μ is 0.7.

(1) Material parameters of Explosive and air.

The structural simulation model used the LS-DYNA ALE method to simulate the impact of the shock wave and the structure.

The JWL [17] equation of state for the explosives was used in the numerical simulation calculation;

$$P = A\left(1 - \frac{\omega}{R_1 V}\right)e^{-R_1 V} + B\left(1 - \frac{\omega}{R_2 V}\right)e^{-R_2 V} + \frac{\omega E}{V}, \tag{2}$$

where P is the pressure of the explosive detonation products; E is the internal energy per unit mass of the explosive; V is the relative volume; and A, B, R_1, R_2, and ω are the material parameters of the explosive. The material parameters and state equation parameters are provided in Tables 1 and 2.

Table 1. Material parameters of the explosives (g-cm-μs).

MID	RO	*D*	P_{CJ}	BETA	*K*	*G*	SIGY
—	1.63	0.693	0.27	0.00	0.00	0.00	0.00

Table 2. Parameters of the explosive (EOS_JWL) (g-cm-μs).

EOSID	*A*	*B*	R_1	R_2	OMEG	E_0	V_0
—	3.71	0.0743	4.15	0.95	0.3	0.07	1.00

(2) Material parameters of Masonry wall

The block bricks and mortar were described by the * MAT 096(MAT_-BRITTLE_DAMAGE) model in LS-DYNA in ANSYS 17.1. This model is primarily an anisotropic brittle damage model for concrete design and can be used for various brittle materials, including bricks and mortar. The restriction on the normal tractions is given by Equation (2) [17]:

$$\phi_t = (n \otimes n) : \sigma - f_n + (1 - \varepsilon) f_n (1 - exp[-H\alpha]) \leq 0 \quad (3)$$

where n is the smeared crack normal, ε is the small constant, f_n is the initial principal tensile strength of the material, H is the softening modulus, and α is an internal variable. Here, H is set automatically by the program; α measures the crack field intensity and is output in the equivalent plastic strain field.

The primary material parameters of block bricks and mortar were listed in Table 3.

Table 3. Material parameters of blocks and mortar.

Material	Density (kg/m^3)	Elastic Modulus/ MPa	Poisson's Ratio	Tensile Strength/ MPa	Shear Strength/ Mpa	Compressive Strength/ Mpa	Fracture Toughness (N/m)	Shear Transfer Coefficient
Block	1150	380	0.15	1.00	0.50	17.6	120	0.03
Mortar	2100	4644	0.25	1.76	0.90	9.0	140	0.03

2.1.2. Numerical Simulation Results

Figure 2 depicts the damage to the wall over time when the TNT was 1 kg. The left and middle figures show that the explosion load first caused a central blasting pit and longitudinal cracks on the blast front surface of the masonry wall and gradually formed divergent cracks along the mortar joint around the blasting pit at about 400 μs. The longitudinal cracks expanded and thickened. The figure on the right suggests that the blast back surface first formed a longitudinal crack, and the central mortar joint of the wall began to crack at 400 μs. As shown in Figure 2c–e, the cracks on the blast back surface show a divergent shape as a whole (except the rib plate).

Figure 3 shows the damage to the wall at t = 1000 μs under different explosive contact weights. The longitudinal cross-sectional view on the left shows that as the amount of charge gradually increased, the depth of the blasting pit increased and cracks were formed. The cracks in the vertical direction of the wall center, i.e., the direction of the axis of symmetry, were particularly deep. The vertical cross-sectional area S of the blasting pit of the brick wall under the contact explosions with different charges showed a gradual increase with increasing charge, and the volume of the blasting pit also showed an increasing trend. The destruction of the middle front surface showed that the strain gradually increased as the amount of charge increased. The area affected by the contact explosion also increased from spherical (Figure 3a) to petaloid (Figure 3b) and to square (Figure 3c,d). The deformation around the blasting pit diverged along the mortar joint in a radial shape (see Figure 3d–h). Sporadic avalanches appeared at the edges of the wall (see Figure 3a–h). The destruction of the back surface on the right side indicated that with the increasing charge, the deformation

range of the back surface gradually increased, and the mortar joint was a weak link. Collapse and spalling also developed along the mortar joint but in the shape of a ring (except the rib plate). The central mortar joint was severely injured, forming a through crack.

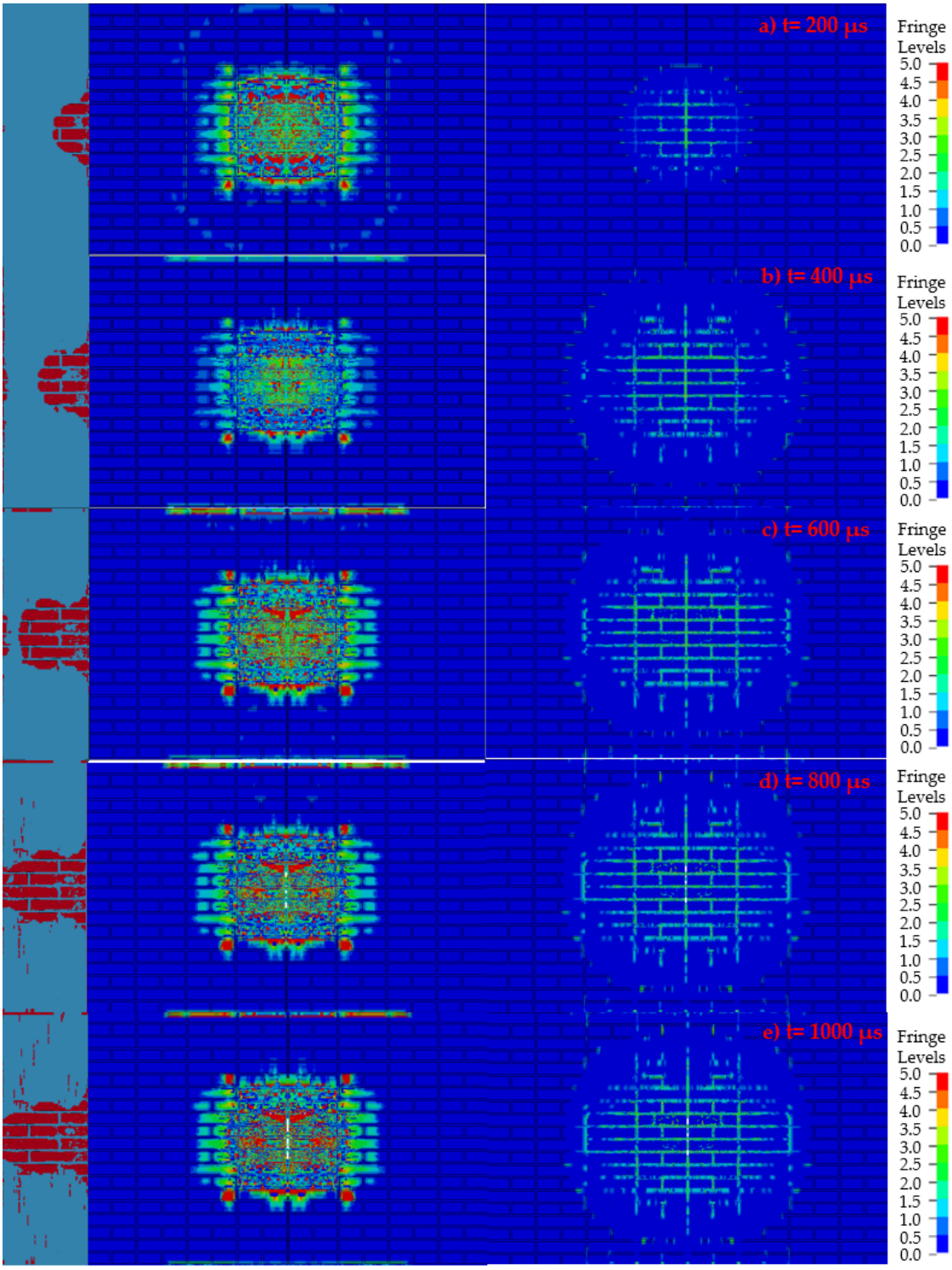

Figure 2. Damage to the 370 mm wall at different times. (**a**) 200 μs; (**b**) 400 μs; (**c**) 600 μs; (**d**) 800 μs; (**e**) 1000 μs.

Figure 4a–c illustrate the linear increases in the area, depth, and radius of the blast pit when the explosive weights increase from 0.25 kg to 1 kg. However, with the increase in

mass of the charge, when the charge is greater than 1 kg, the area, depth, and radius of the explosive pit increase slowly and tend to be horizontal. This means that the charge mass of 1 kg is a critical state, and the damage form changes when it exceeds 1 kg.

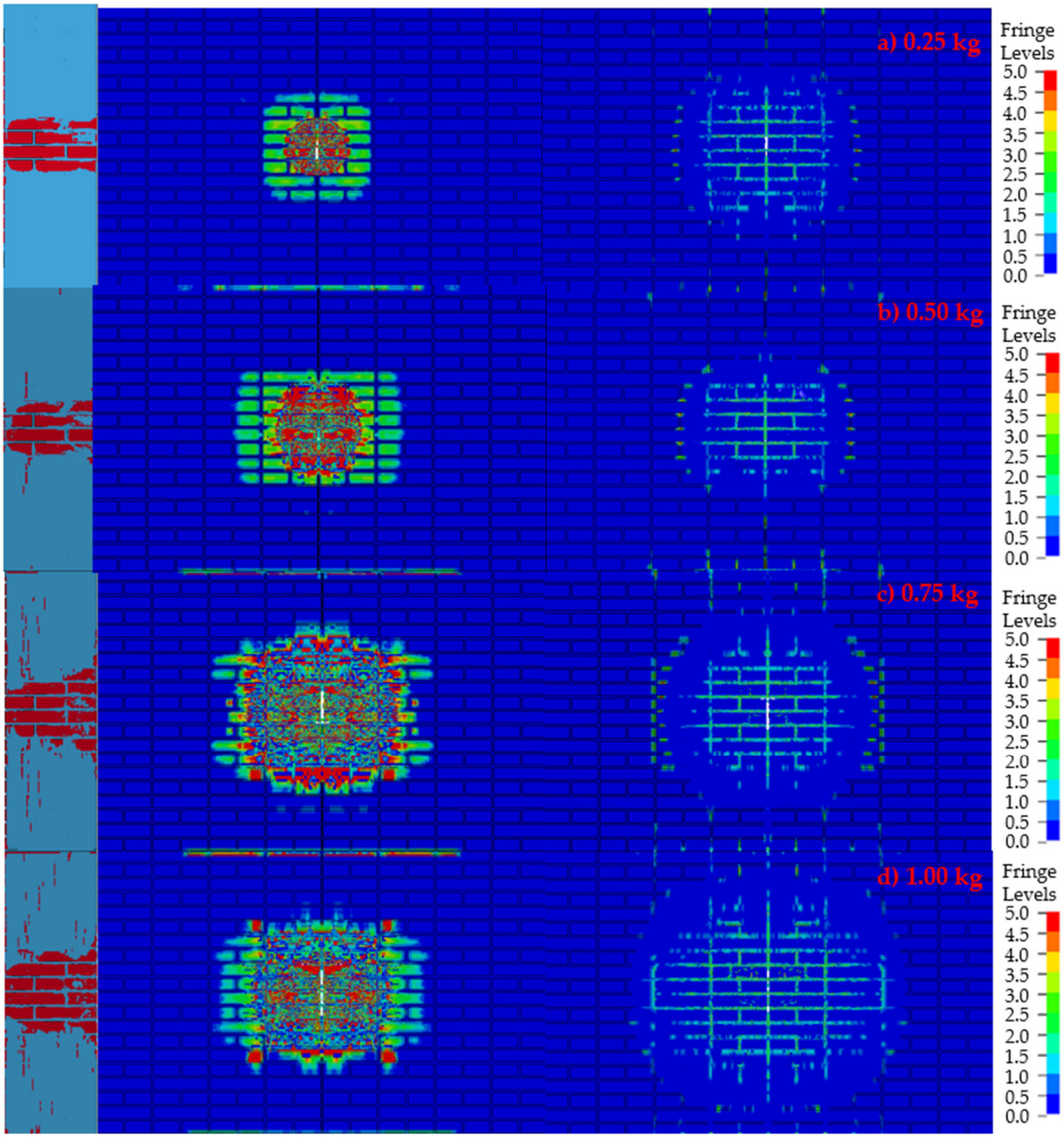

Figure 3. *Cont.*

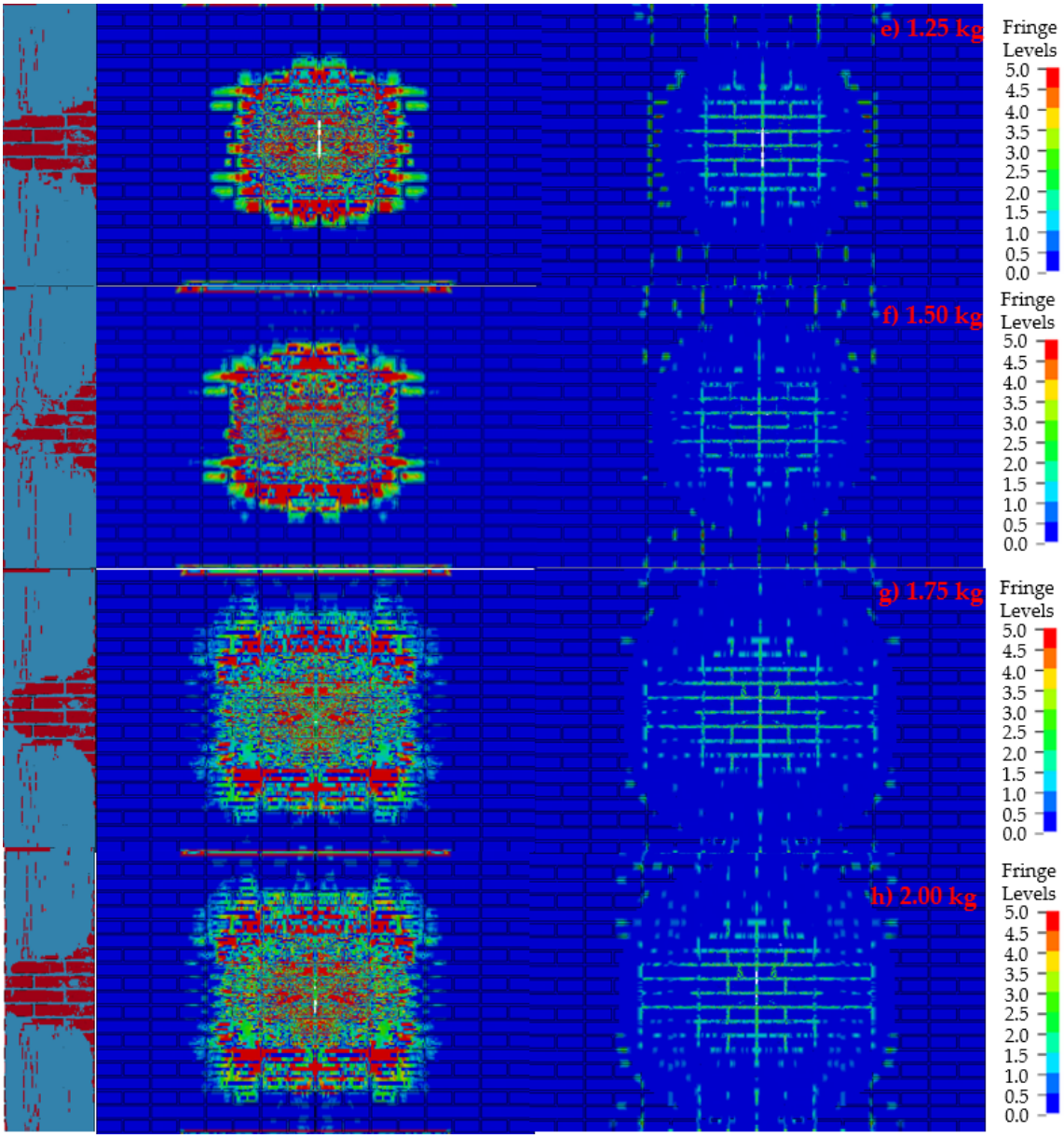

Figure 3. Damage to the 370 mm wall under different weights of TNT. (**a**) 0.25 kg; (**b**) 0.50 kg; (**c**) 0.75 kg; (**d**) 1.00 kg; (**e**) 1.25 kg; (**f**) 1.50 kg; (**g**) 1.75 kg; (**h**) 2.00 kg.

2.2. Blast-Resistant Characteristics of Masonry Wall Sprayed with Polyurea Elastomer

In this section, we detail the numerical simulations of the blast-resistant characteristics of masonry walls sprayed with different thicknesses of a polyurea elastomer.

2.2.1. Numerical Model

In the numerical simulation, the thickness of the polyurea reinforcement layer on the front surface remained unchanged at 6 mm, while the thickness of the back surface reinforcement layer was changed to study the influence of the thickness changes in the polyurea reinforcement layer on the failure of the masonry wall under contact explosion. The thickness of the polyurea reinforcement layer of the 370 mm wall model is shown in Table 4. The 1/2 model of the sprayed polyurea-reinforced 370 mm wall and the meshing of the large-scale surface of the polyurea coating are shown in Figure 5. The bonding force between the polyurea elastomer and the brick wall was obviously greater than the peel strength of the mortar, so the polyurea elastomer sprayed on the surface of

the clay masonry wall and the wall were coupled by a common node to simulate their deformation coordination.

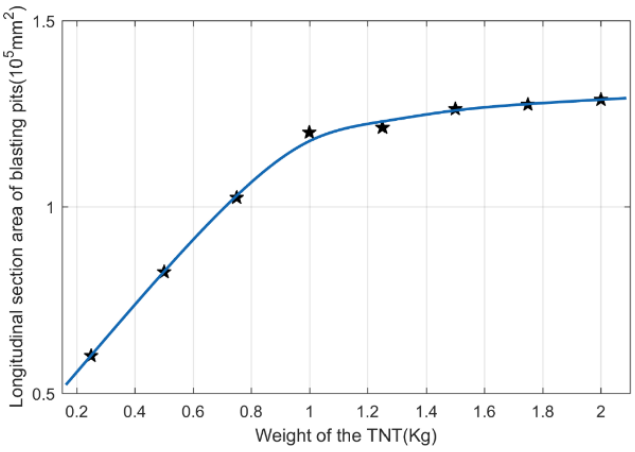

(**a**)

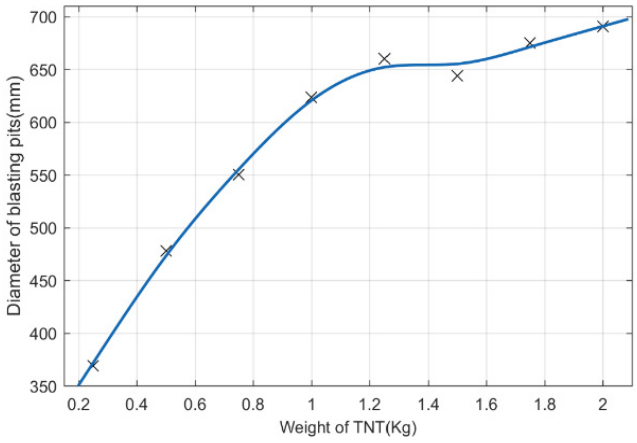

(**b**)

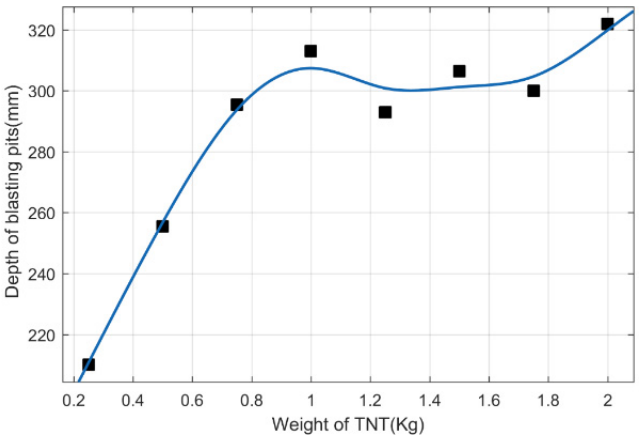

(**c**)

Figure 4. Statistics for the longitudinal section size of the 370 mm wall under different weights of TNT: (**a**) longitudinal section area of the blasting pits; (**b**) diameter of the blasting pits; (**c**) depth of the blasting pits.

Table 4. Thickness dimensions of the polyurea reinforcement layer of a 370 mm wall model.

Serial number	1	2	3	4
Polyurea thickness on back surface/mm	2	4	6	8

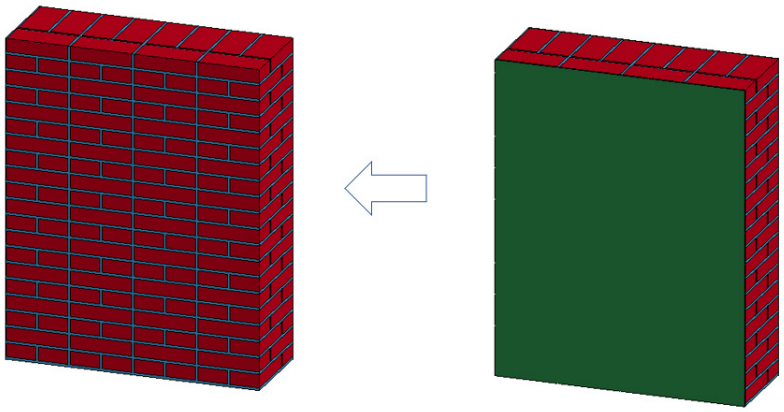

Figure 5. The 1/2 finite element model of the sprayed polyurea-strengthened 370 mm wall and the meshing of the polyurea layer.

Table 5 shows the mechanical properties of the polyurea elastomer [18].

Table 5. Parameters of the polyurea elastomer.

E/GPa	ρ/(g/cm^3)	ν	σ_Y/GPa	E_Y/GPa	σ_0/GPa
230	**1.02**	**0.4**	**1.38**	**3.50**	**13.8**
Load curve 1			Load curve 2		
1.0×10^{-1}	2.3×10^{-4}		1.6×10^{-9}	5.0×10^{-5}	
3.0×10^{-1}	2.7×10^{-4}		1.6×10^{-7}	6.0×10^{-5}	
5.0×10^{-1}	3.5×10^{-4}		1.4×10^{-5}	8.0×10^{-5}	
8.0×10^{-1}	4.2×10^{-4}		8.0×10^{-5}	8.5×10^{-5}	
8.5×10^{-1}	4.9×10^{-4}		8.0×10^{-4}	1.1×10^{-4}	
9.0×10^{-1}	5.8×10^{-4}		2.25×10^{-3}	1.2×10^{-4}	
			16.5×10^{-3}	1.6×10^{-4}	
			9.0×10^{-3}	2.2×10^{-4}	

2.2.2. Numerical Simulation of the Polyurea-Reinforced 370 mm Wall

When the amount of TNT was 1 kg under working condition 2 (the thickness of the reinforcement layer on the front surface was 6 mm and the thickness of the reinforcement layer on the back surface was 4 mm), Figure 6 illustrates the 370 mm wall's damage over time. The figure on the left shows the front side of the reinforced wall before the explosion, which reflects the damage to the surface of the polyurea reinforcement layer before the explosion. The middle figure is only the stress cloud diagram of the wall, reflecting the damage of the inner wall of the masonry. The figure on the right shows the rear side of the reinforced wall after blasting, reflecting the damage to the polyurea reinforcement layer on the blasted surface.

From the front view on the left, after the contact explosion, the polyurea layer on the front surface stretched and dented quickly under the action of the explosion load and was quickly damaged to expose the masonry wall structure of the lower layer. The polyurea layer at the central symmetry plane showed wavy distortion (see Figure 6a). The breach of the polyurea layer on the blast front face expanded rapidly with time, and the polyurea layer around the breach was stacked and folded after extrusion and stretching (see Figure 6a–d). After 800 μs, when the central breach of the polyurea layer expanded to

a certain extent, the size growth slowed down and some near-circular bulges appeared on the periphery of the stacked fold layer of the breach, leading to the uneven periphery of the folds (see Figure 6d,e).

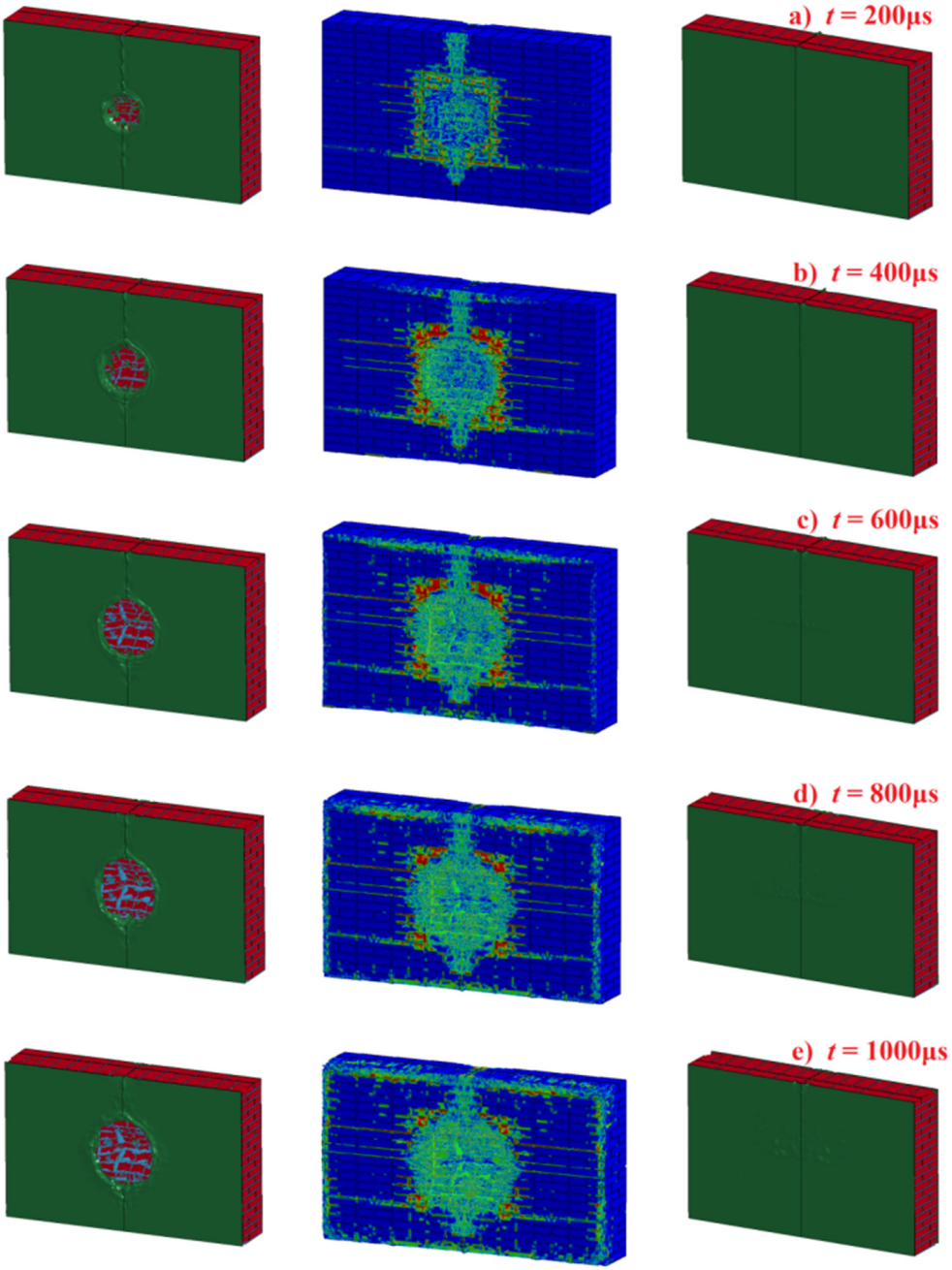

Figure 6. Destruction of the polyurea-reinforced 370 mm wall at different times. (**a**) 200 μs; (**b**) 400 μs; (**c**) 600 μs; (**d**) 800 μs; (**e**) 1000 μs.

Based on the stress diagram of the brick masonry in the middle, the explosive load first caused a rapidly expanding central blasting pit and large longitudinal cracks on the front surface of the masonry wall, with some divergent cracks formed along the mortar joint around the blasting pit (see Figure 6a). After 400 μs, the area and volume of the central blasting pit increased, radial cracks around it developed and were densely distributed, and the upper and lower sides of the wall were damaged (see Figure 6b,c). After 800 μs, the increase in size of the central blasting pit was no longer obvious, and a little peeling damage also appeared on the left and right sides of the wall (see Figure 6d,e). Based on a

comparison of the figures on the left and in the middle, the area of the polyurea elastomer coating breach was always smaller than the area of the central blasting pit sandwiched by the masonry wall at any time.

The back surface on the right showed that the explosion load caused large longitudinal cracks in the center of the wall on the back surface, resulting in slight distortion in the top and middle of the back polyurea reinforcement layer (see Figure 6a,b). From 600 μs, the middle gray seam of the polyurea reinforcement layer on the back surface gradually showed lumpy protrusions under the action of impact waves, and the raised lumps merged with each other and expanded (see Figure 6c–e).

Figure 7 shows the damage to the polyurea reinforcement layer on both sides under contact explosion at t = 1000 μs. The back surface reinforcement layer has thickness *k* values of 2, 4, 6, and 8 mm, which correspond to the damage of working conditions 1–4, respectively, as shown by labels a through d. The figure on the left is the front surface of the reinforced wall, reflecting the damage of the polyurea reinforcement layer on the front surface; the figure on the right is the back side of the wall, reflecting the damage of the polyurea reinforcement layer on the back surface. Based on the front surface on the left under the same contact explosion load, the levels of deformation of the reinforcement layers from the explosions on the surfaces of the same thickness were very similar. The wavy distortions of the central symmetry plane were similar, and the sizes of the openings were almost the same. The polyurea layers around the break showed similar stacking, folding, and bulging after extrusion and stretching.

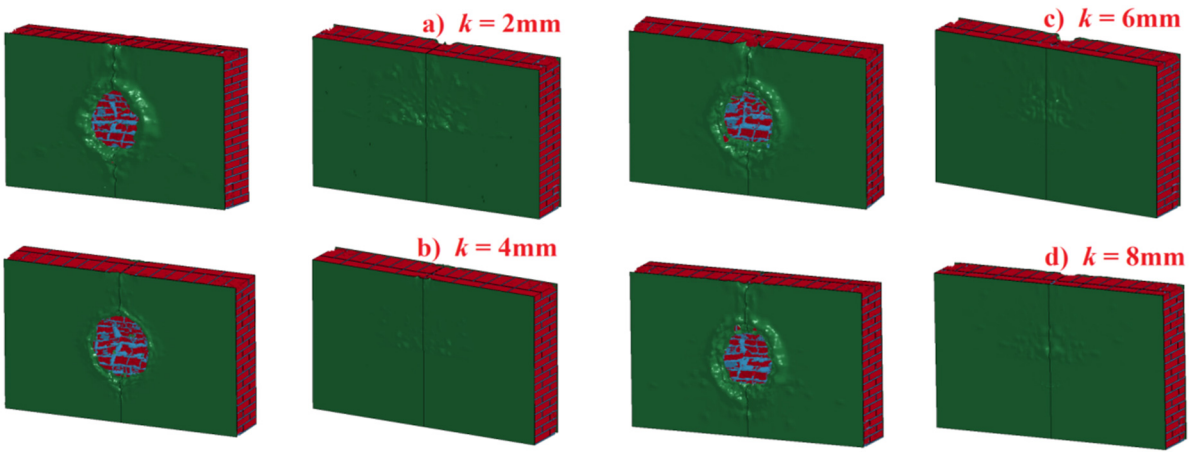

Figure 7. Damage of polyurea reinforcement layer under contact explosion at 1000 μs with different *k* values (thickness of the back face): (**a**) k = 2 mm; (**b**) k = 4 mm; (**c**) k = 6 mm; (**d**) k = 8 mm.

Based on the back surface on the right, when the polyurea reinforcement layer on the back surface was thin (i.e., in working conditions 1 and 2, as shown in Figure 7a,b), the distortion of the top and middle parts of the reinforcement layer was obvious, and the uplift of the reinforcement layer was small and dense, often distributed along the mortar joint. When the polyurea reinforcement layer was thick (i.e., in working conditions 3 and 4, as shown in Figure 7c,d), the distortion of the top and middle parts of the reinforcement layer was not obvious, and the uplifts of the reinforcement layer were larger but smaller in number, distributed in the corresponding central part of the blasting pit.

To more clearly see the damage to the reinforced masonry wall under contact explosions, Figure 8 was created without the polyurea reinforcement layers on each side. Only the damage to the bricks and mortar under the four working conditions in Table 4 is depicted in the image. The reinforced masonry wall's longitudinal section or symmetrical plane, blast front surface, and blast back surface are all destroyed on the figure's left, middle, and right sides, respectively.

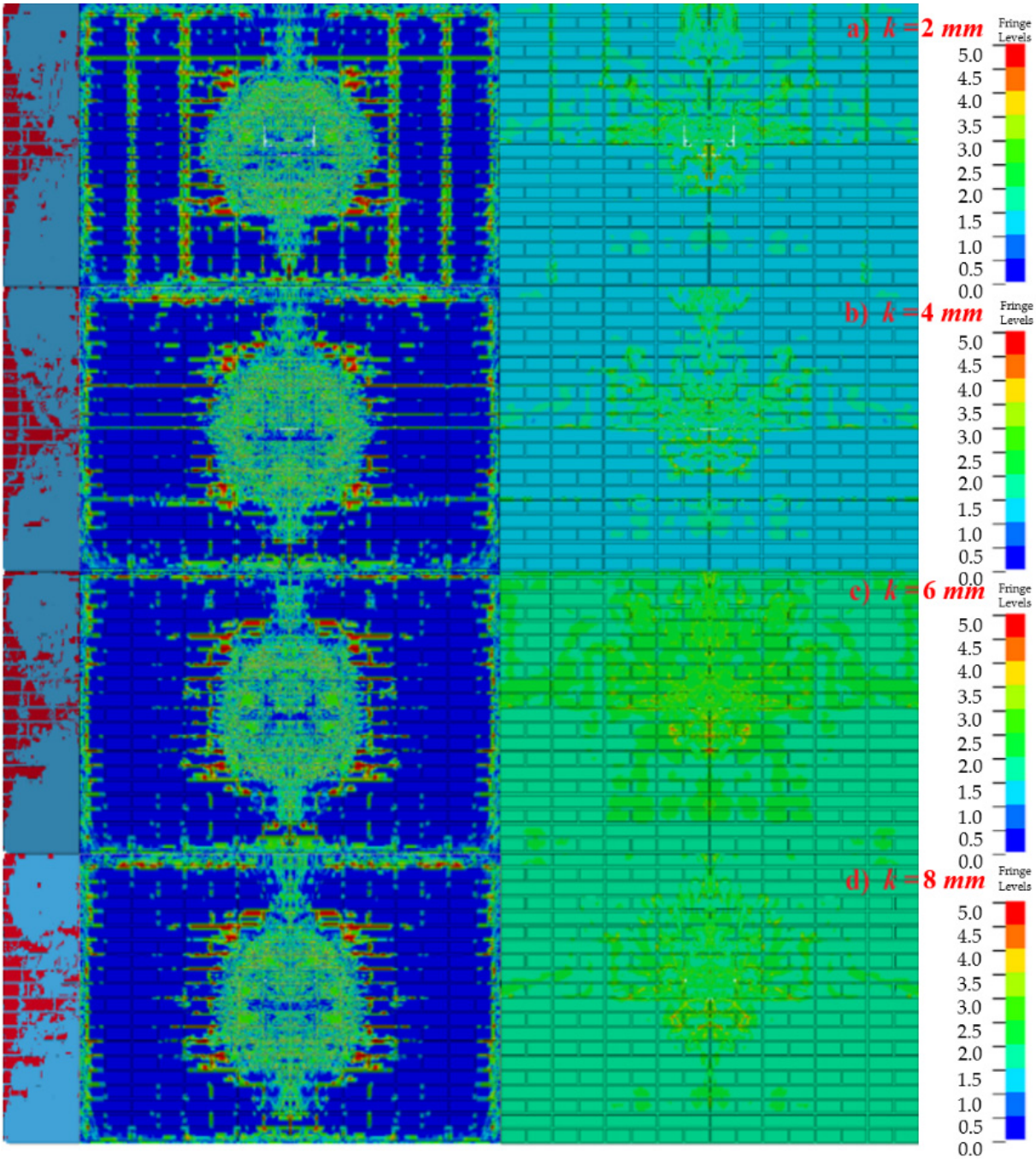

Figure 8. Damage to the reinforced 370 mm wall under contact explosion at 1000 μs with different *k* values (thickness of back face: (**a**) k = 2 mm; (**b**) k = 4 mm; (**c**) k = 6 mm; (**d**) k = 8 mm.

As shown in the longitudinal section on the left, when the thickness of the polyurea reinforcement layer on the front surface remained unchanged, the depth of the central blasting pit of the masonry wall did not change much with the increasing thickness of the back surface reinforcement layer, and the cracks were densely distributed inside the masonry wall. The damage to the front surface in the middle shows that the areas of the central blasting pit (circled in the figure) under the four working conditions were different. When the back surface was thin (i.e., in conditions 1 and 2, as shown in Figure 8a,b), the area of the blasting pit was larger. When the polyurea reinforcement layer was thicker (i.e., in conditions 3 and 4, as shown in Figure 8c,d), the area of the blasting pit was smaller; the spalling and cracking of the explosion-proof surface of the wall under the four working

conditions were also different. Compared with conditions 3 and 4, the damage phenomena, such as the spalling and cracks on the blast front surface of the masonry wall concentrated in the mortar joint in conditions 1 and 2, were more obvious. The damage to the back surface on the right shows that under the four working conditions, the mortar joints were all weak links, and the collapse and spalling developed along the joints, with an overall radial trend (except for the rib plate). Compared with working conditions 3 and 4, where the polyurea reinforcement layer on the back surface was thicker, the strain on the back surface of the masonry wall in working conditions 1 and 2 was smaller.

By selecting the damaged areas along the bounding box, the size statistics of the same wall with different reinforcement methods under the same contact explosion load are shown in Table 6. As the thickness of the polyurea elastomer reinforcement layer on the blast back surface increased, the area of the central blasting pit decreased slightly; the values of working conditions 1 and 2 were close to those of working conditions 3 and 4. With the increasing thickness of the polyurea reinforcement layer on the blast back surface, the overall depth of the blasting pit did not change much, whereby the depths for working conditions 1, 2, and 4 were quite close, at about half of the thickness of the masonry wall.

Table 6. Size statistics for the destruction of the reinforced 370 mm wall under contact explosion.

Serial Number	Thickness of Front Surface/mm	Thickness of Back Surface/mm	Burst Area/mm^2	Burst Depth/mm
1	6	2	388,654	201
2	6	4	380,232	199
3	6	6	353,282	236
4	6	8	339,903	203

3. Experiment

3.1. Experimental Verification of 370 mm Wall under Contact Explosions

3.1.1. Test Plan and Arrangement

The test wall size was 2000 mm × 1200 mm × 370 mm, and a pair of ribs were symmetrically arranged on both sides of the wall to simulate the supporting effect of the surrounding walls on the actual building. The wall surface was smoothed with about 2 mm of mortar. The explosive used in the test was a TNT cylindrical compressed explosive with a charge density of 1.63 g/cm^3. Two charge specifications were used, i.e., 0.50 kg (test 1) and 1.00 kg (test 2). The basic dimensions were Φ100 mm × 39 mm and Φ100 mm × 78 mm. The wall was larger than the explosive to ensure that the explosive would not destroy the entire wall and to avoid the influence of the masonry wall and the size effect of the charge. Tests 1 and 2 correspond to the b and d working conditions in the numerical simulation, respectively. The test layout is shown in Figure 9.

Figure 9. Test layout.

3.1.2. Experimental Results and Analysis

The experimental results and measured parameters are shown in Figure 10. In Figure 10a, a blasting pit is shown in the center of the blast front surface of the masonry wall. Most of collapse damage occurred in the mortar position, resulting in a small amount of block fragments, and the fragments scattered outwards. The fragments fell below the blasting pit, and the fragments were all over the area in front of the test wall. Large cracks appeared on the left and right sides and the upper side of the blasting pit on the front surface of the wall in the horizontal direction. The cracks penetrated to the back surface of the masonry wall. Small spidery radioactive spalls appeared around the blasting pit on the front surface. In test 2, a large blasting pit appeared in the center of the front surface of the masonry wall (see Figure 10b–d). The collapse damage also mostly appeared in the mortar, resulting in large amounts of block fragments and flying debris. Large penetrating cracks appeared in the horizontal direction and upper side of the blasting pit on the front surface of the wall. The upper left part of the masonry wall collapsed backward along the large cracks, and the upper right part was staggered along the large cracks and deflected at a small angle of about 2.3°.

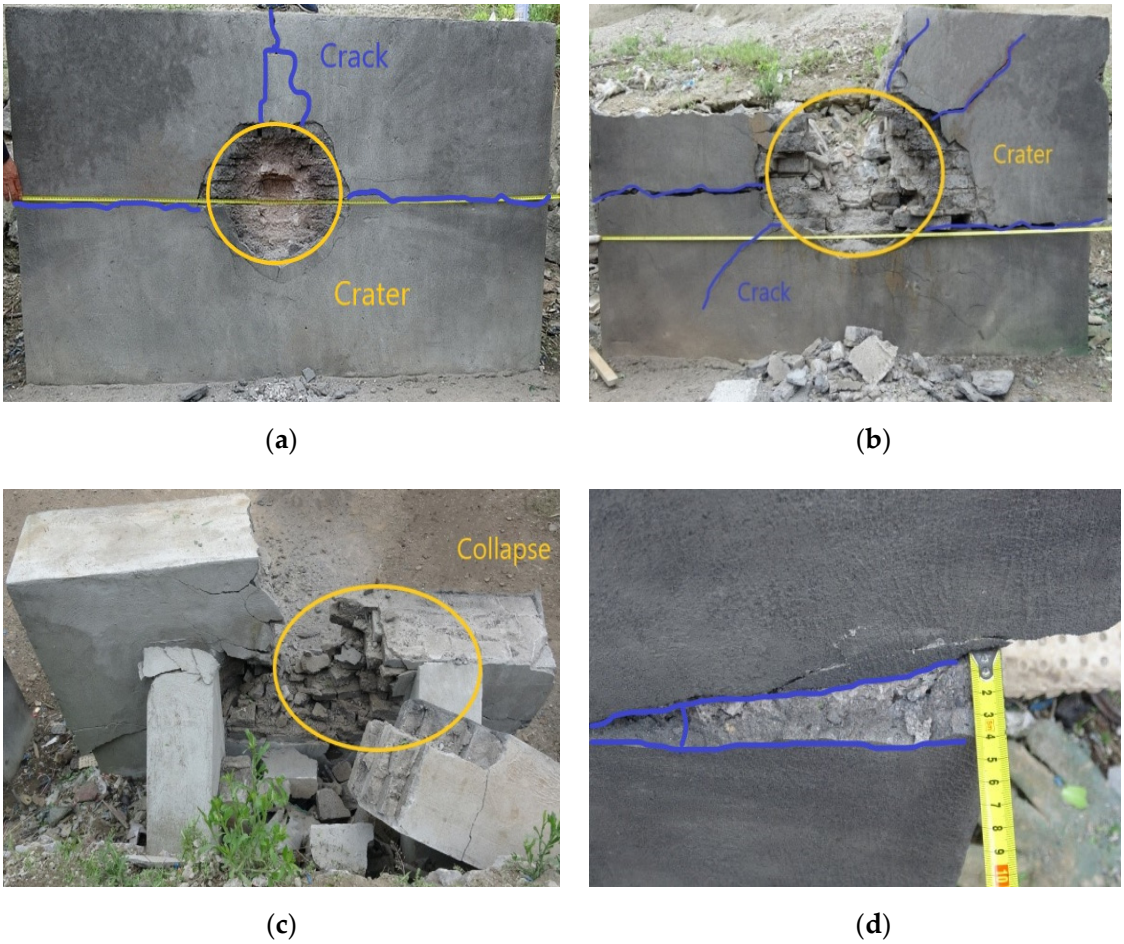

(**a**) (**b**)

(**c**) (**d**)

Figure 10. Damage of the wall in the test. (**a**) Test 1 blast front surface; (**b**) Test 2 blast front surface; (**c**) Test 2 blast back surface; (**d**) Test 2 Wall deflection.

3.2. Experimental Verification of Sprayed Polyurea to Reinforce 370 mm Wall under Contact Explosion

3.2.1. Test Plan and Arrangement

The masonry wall was the same as in the prior part, and a polyurea spray was utilized as the reinforcement. The TNT explosive with a density of 1.63g/cm^3, a mass of 1 kg, and

dimensions of 100 mm × 78 mm was employed in the test. The reinforced 370 mm wall was sprayed with a 6-mm-thick polyurea reinforcement coating on the blast front surface and 2-mm- and 4-mm-thick polyurea reinforcement layers on the rear surface, respectively. Tests 1 and 2 correspond to working conditions 1 and 2 in the simulation, respectively, and the layout of the test site is shown in Figure 11.

Figure 11. Test site layout.

3.2.2. Experimental Results and Analysis

Figure 12 displays the damage to the reinforced wall during the test. The polyurea elastomer reinforcement layer coated on the surface was removed while maintaining the damaged state of the wall as much as possible. The right side of t figure demonstrates the damage to the wall when the reinforcing layer was removed. In tests 1 and 2, the center of the front surface in Figure 12a,b produced a hole with a small diameter, and on both sides of the hole there were several short tears. The area between the polyurea reinforcement layer and the brick wall "caught" some of the wall fragments, trash, and dust, which was visible through the hole in the reinforcement layer. Large blasting pits with shallow edges were formed in the center of the internal masonry wall, but the depth of the pits became larger in the part corresponding to explosive position. A large number of large radial cracks were distributed around the blast pit, with horizontal and vertical cracks penetrating the brick wall. In test 2, around the center blasting hole of the interior masonry wall, numerous little spidery fractures and spalls appeared along the mortar joints. Based on Figure 12c, the large cracks in the wall center of test 2 extended to the back surface, and the back surface of the internal masonry wall had cracks diverging from the center to the surroundings, where the horizontal and vertical cracks were the coarsest. The polyurea elastomer reinforcing layer on the blast back surface was not torn by massive fractures though. The reinforcing layer, which experienced a minor uplift under the displacement of the internal brick wall, blocked the huge fractures on top, as seen in the left half of Figure 12c.

(**a**)

Figure 12. *Cont.*

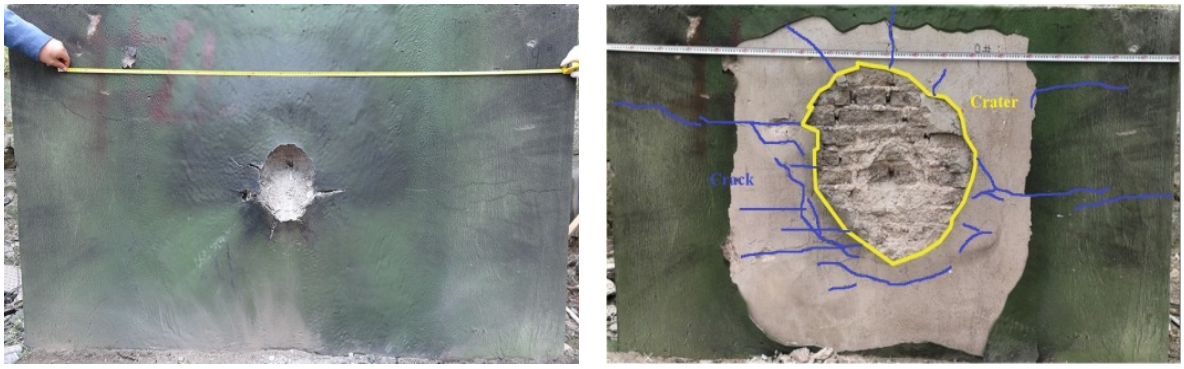

(**b**)

(**c**)

Figure 12. Damage to the reinforced 370 mm wall in the test. (**a**) Test 1 blast front surface; (**b**) Test 2 blast front surface; (**c**) Test 2 blast back surface.

4. Comparative Analysis

4.1. Comparative Analysis of Numerical Simulation and Experimental Results for an Unreinforced Wall

The numerical simulation showed that when the charge was less than 1 kg, blasting pits and longitudinal cracks predominated; when the charge was greater than 1 kg, the wall's front surface was covered in cracks and its back surface was covered in annular cracks along the mortar joint. In the test, the small charge in test 1 only formed blasting pits and a few cracks. However, not only did the increased charge in test 2 form larger blasting pits and thicker cracks, the complete penetration of the cracks also led to the brittle fracture of the wall. As such, dislocation, deflection, and collapse occurred under the action of the impact wave.

When the contact explosion occurred, the expansion wave and impact wave of the detonation products immediately reached the masonry wall, and the compressive stress wave caused serious damage to the front face of the wall. The central blasting pit and its surrounding cracks developed to different thicknesses along the mortar joint. The pressure surge propagated to the blast back surface to form a strong tensile wave, which caused the collapse and spalling of the back surface. The collapse and spalling caused by the strong tensile wave also developed along the mortar joint in a circular trend, forming penetrating cracks at the central mortar joint.

As shown in Figure 3, after the charge quantity exceeded 1 kg, the expansion of the blasting pit size gradually came to an end. According to the dislocation and collapse of the masonry wall in test 2, when the charge was large, the wall was penetrated and the energy of blast was converted into the displacement part of the wall. The dominant mode of energy release for the masonry wall changed as the charge increased; that is, when the charge was less than 1 kg, the damage to the masonry wall by explosives was mainly reflected in the cross-shaped cracks in the central blasting pits and in horizontal and vertical directions, and then when the charge exceeded 1 kg, the wall was penetrated and the damage to

the masonry wall gradually spread, especially the damage to the surrounding mortar joints, until part of the mortar joints penetrated the wall and caused the wall's dislocation, deflection, and collapse.

4.2. Comparative Analysis of Numerical Simulation and Experimental Results for a Reinforced Wall

When the reinforced masonry wall was subjected to the contact explosion load, the numerical simulation depicted the process of large blasting pits forming, with small cracks forming at the edge of the pits and growing along the mortar joints, and coarse cracks gradually extending and even penetrating along the mortar joints in the horizontal and vertical directions. The general consistency of the damage state with the test results shows that the wall model with the polyurea reinforcement layer and the polyurea material model can accurately represent the dynamic response of a reinforced masonry wall under contact explosion load.

In the numerical simulation of the reinforced 370 mm wall, the depths of the blasting pits in the four working conditions were close. When the polyurea reinforcement layer on the back surface was thin, the deformation mainly appeared as the collapse of the masonry around the blasting pits and large-area cracks that developed along the mortar joints, except for in the central blasting pit. When the thickness of the polyurea reinforcement layer on the blast back surface was thick, the crack damages on the front surface of the wall converged.

Compared with the unreinforced 370 mm wall under a 1 kg TNT contact explosion (see Figure 3b–d), the damage to the masonry wall reinforced by the polyurea elastomer under the two working conditions was improved under the same conditions. After reinforcement, the cracks on the surface and other minor damages to the masonry wall increased. The blasting area of test 2 was significantly larger than that of the unreinforced wall, but the number of thick cracks penetrating the 370 mm wall was significantly reduced, with only the longitudinal cracks in the middle remaining. More importantly, the unreinforced masonry, which suffered severe penetrating damage under the contact explosion in the upper part of the wall, deflected and even collapsed, and large amounts of wall fragments, debris, and dust were scattered around the wall after splashing. After spraying the polyurea elastomer for reinforcement, the depth of the central blasting pit was suppressed effectively, the masonry wall remained complete under the contact explosion load, and the polyurea reinforcement layer on the blast back surface of the wall wrapped the debris generated by the wall damage effectively and prevented the splashing of the debris and other destructive elements.

Table 7 shows a simulation and test parameter comparison of the damages to the unreinforced 370 mm wall and the 370 mm wall reinforced by spraying the polyurea elastomer under contact explosion. The areas of the central blasting pit after reinforcement were all larger than those of the unreinforced 370 mm wall. With the increasing thickness of the polyurea reinforcement layer on the blast back surface, the area of the blasting pit slightly reduced; the blasting area in test 2 was close to the numerical simulation value (the error was about 10.3%), but the blasting area in test 1 was quite different from the numerical simulation value. The manually sprayed polyurea layer on the brick wall in the test was not uniform, leading to a certain degree of variation in the test results. Before the explosion test, the wall in the explosion test site of test 1 was improperly stored, and the polyurea reinforcement layer at the lower left corner was damaged and partially peeled off (see Figure 12a), causing a break in the lower left corner. Although the break was at the edge of the wall and far from the center of the contact explosive load, the break acted as a "vent." The right figure in Figure 12a shows that from the surroundings of the central blasting pit to the lower left corner, black detonation product residue was left on the masonry wall, which reduced the surface damage to the masonry wall in test 1 and decreased the area of the blasting pit.

Table 7. Comparison of the parameters for the destruction of the reinforced 370 mm wall under contact explosion.

Serial Number	Polyurea Thickness on Front Surface/mm	Polyurea Thickness on Back Surface/mm	Blasting Area/mm^2		Blasting Depth/mm	
			Numerical Simulation	Experimental Validation	Numerical Simulation	Experimental Validation
Unreinforced	0	0	292,247	—	315	Penetrated
Working condition 1/test 1	6	2	388,654	271,847	201	191
Working condition 2/test 2	6	4	380,232	344,577	199	196
Working condition 3	6	6	353,282	—	236	—
Working condition 4	6	8	339,903	—	203	—

Table 7 shows that the depth of the central blasting pit after reinforcement was less than the corresponding value of the unreinforced 370 mm wall. The simulation values for working conditions 1, 2, and 4 were close. Compared with the unreinforced 370 mm wall, the depth of blasting pit reduced significantly to about 36.4%. The numerical simulation values of blasting pit depths for working conditions 1 and 2 were in good agreement with the experimental values, with errors of 5.1% and 1.4%, respectively.

In summary, for working condition 1, the depth of the central blasting pit of the 370 mm wall was suppressed effectively, and the scattering of fragments, debris, and other destructive elements was prevented, thereby greatly improving the support and integrity of the wall. For working conditions 2 to 4, although a certain blast-resistant effect was achieved, the doubling of the thickness of polyurea layer on the back surface did not significantly increase the corresponding blast-resistant effect. Therefore, when the polyurea layer on the front explosion surface of the 370 mm wall was fixed at 6 mm, a coating of 2 mm of polyurea elastomer on the blast back surface can achieve a good reinforcement effect.

5. Conclusions

The following conclusions were reached after an analysis of the failure characteristics and damage processes of unreinforced and reinforced masonry walls under contact explosions:

(1) The destructional forms of the masonry wall under the contact explosions can be grouped into two kinds. When the explosive charge was below the critical value, the destruction of the masonry wall occurred near the explosive, forming a central blasting pit, a penetrating hole, and cross-cracks oriented in both horizontal and vertical directions. The other form of destruction slowly spread to the surrounding area, particularly the mortar joints; the spalling and collapse of the blast back surface also increased noticeably, meaning that eventually the wall would fall;

(2) The critical value of the TNT explosive for the 370 mm masonry wall under contact explosion was 1 kg. When the TNT explosive was over 1 kg, the destructional form of the masonry wall involved the splashing of wall fragments, deflection, and movement of the wall after the explosion;

(3) The polyurea elastomer sprayed on the front surface of the masonry wall can attenuate the shock waves generated by the TNT explosions effectively, and the polyurea elastomer sprayed on the back surface of the masonry wall can effectively restrain the wall breakage after the explosion. When the masonry wall was sprayed with the elastomer on the front and back surfaces, the wall's resistance to the damage caused by the explosive increased;

(4) When the thickness of the front polyurea layer was 6mm and the thickness of the back polyurea layer was 2 mm, the masonry wall had the best blast-resistant effect.

Author Contributions: Conceptualization, Q.X.; methodology, X.Z. and Z.H.; validation, Z.H.; test, Q.X., X.Z., and Z.H.; writing—original draft preparation, X.Z.; writing—review and editing, Y.C. and T.C. All authors have read and agreed to the published version of the manuscript.

Funding: This research was funded by the National Natural Science Foundation of China (grant No. 11872214).

Institutional Review Board Statement: Not applicable.

Informed Consent Statement: Not applicable.

Data Availability Statement: The data are contained within this article; more detailed data can be obtained from the corresponding author.

Conflicts of Interest: The authors declare no conflict of interest.

References

1. Porter, J.; Dinan, R.; Hammons, M.; Knox, K. Polymer coatings increase blast resistance of existing and temporary structures. *Amptiac Q.* **2002**, *6*, 47–52.
2. Davidson, J.; Porter, J.R.; Dinan, R.; Hammons, M.; Connell, J.D. Explosive testing of polymer retrofit masonry walls. *J Perform. Constr. Facil.* **2004**, *18*, 100–106. [CrossRef]
3. Bahei-El-Din, Y.A.; Dvorak, G.J.; Fredricksen, O.J. A blast-tolerant sandwich plate design with a polyurea interlayer. *Int. J. Solids Struct.* **2006**, *43*, 7644–7658. [CrossRef]
4. Tekalur, S.A.; Shukla, A.; Shivakumar, K. Blast resistance of polyurea based layered composite materials. *Compos. Struct.* **2008**, *84*, 271–281. [CrossRef]
5. Hrynyk, T.D.; Myers, J. Out-Of-Plane behavior of URM arching walls with modern blast retrofits: Experimental results and analytical model. *J. Struct Eng.* **2008**, *134*, 1589–1597. [CrossRef]
6. Aghdamy, S.; Wu, C.; Griffith, M. Simulation of Retrofitted Unreinforced Concrete Masonry Unit Walls under Blast Loading. *Int. J. Prot. Struct.* **2013**, *4*, 21–44. [CrossRef]
7. Davidson, J.S.; Fisher, J.W.; Hammons, M.I.; Porter, J.R.; Dinan, R.J. *Failure Mechanisms of Polymer-Reinforced Concrete Masonry Walls Subjected to Blast*; Air Force Research Laboratory Tyndall Air Force Base: Bay County, FL, USA, 2005.
8. Gattesco, N.; Boem, I. Out-of-plane behavior of reinforced masonry walls: Experimental and numerical study. *Compos. Part B Eng.* **2017**, *128*, 39–52. [CrossRef]
9. Fan, J.Y.; Fang, Q.; Zhang, Y.D. Numerical simulation on the anti-blast properties of masonry walls. *Prot. Eng.* **2011**, *33*, 35–40.
10. Guo, Y.R.; Zheng, H. Numerical Simulation of Polyurethane Strengthened Perforated Masonry Walls under Blast Loading. In *Advanced Materials Research*; Trans Tech Publications Ltd.: Wollerau, Switzerland, 2013.
11. Xu, K.; Lu, Y. Numerical simulation study of spallation in reinforced concrete plates subjected to blast loading. *Comput. Struct.* **2006**, *84*, 431–438. [CrossRef]
12. Dinan, R.; Fisher, J.; Hammons, M.I.; Porter, J.R. *Failure Mechanisms in Unreinforced Concrete Masonry Walls Retrofitted with Polymer Coatings*; Air Force Research Laboratory Tyndall Air Force Base: Bay County, FL, USA, 2003.
13. Zhu, H.; Wang, X.; Wang, Y.; Ji, C.; Wu, G.; Zhang, L.; Han, Z. Damage behavior and assessment of polyurea sprayed reinforced clay brick masonry walls subjected to close-in blast loads. *Int. J. Impact Eng.* **2022**, *167*, 104283. [CrossRef]
14. Iqbal, N.; Sharma, P.; Kumar, D.; Roy, P. Protective polyurea coatings for enhanced blast survivability of concrete. *Constr. Build. Mater.* **2018**, *175*, 682–690. [CrossRef]
15. Ji, L.; Wang, P.; Cai, Y.; Shang, W.; Zu, X. Blast Resistance of 240 mm Building Wall Coated with Polyurea Elastomer. *Materials* **2022**, *15*, 850. [CrossRef] [PubMed]
16. *GB 50003-2011*; Code for Design of Masonry Structures. General Administration of Quality Supervision, Inspection and Quarantine of the People's Republic of China: Beijing, China, 2011.
17. Hallquist, J.O. *LS–DYNA Keyword User's Manual*; Livemore Software Technology Corporation: Livermore, CA, USA, 2007.
18. Gan, Y.-D.; Song, L.; Yang, L.-M. Numerical Simulation for Anti-blast Performances of Steel Plate Coated with Elastomer. *Binggong Xuebao/Acta Armamentarii* **2009**, *30*, 15–18.